

## Self-consistency and sum-rule tests in the Kramers-Kronig analysis of optical data: Applications to aluminum

E. Shiles\*

*Argonne National Laboratory, Argonne, Illinois 60439*

Taizo Sasaki

*University of Tokyo, Komaba, Tokyo 153, Japan*

Mitio Inokuti and D. Y. Smith

*Argonne National Laboratory, Argonne, Illinois 60439*

(Received 2 January 1980)

An iterative, self-consistent procedure for the Kramers-Kronig analysis of data from reflectance, ellipsometric, transmission, and electron-energy-loss measurements is presented. This procedure has been developed for practical dispersion analysis since experimentally no single optical function can be readily measured over the entire range of frequencies as required by the Kramers-Kronig relations. The present technique is applied to metallic aluminum as an example. The results are then examined for internal consistency and for systematic errors by various optical sum rules. The latter provide tests of agreement with both theoretical constraints and independently measured properties such as electron density, dc conductivity, and stopping power. The present procedure affords a systematic means of preparing a self-consistent set of optical functions provided some optical or energy-loss data are available in all important spectral regions. The analysis of aluminum discloses that currently available data exhibit an excess oscillator strength, apparently in the vicinity of the  $L$  edge. A possible explanation is a systematic experimental error in the absorption-coefficient measurements resulting from surface layers—possibly oxides—present in thin-film transmission samples. A revised set of optical functions has been prepared by an *ad hoc* reduction of the reported absorption coefficient above the  $L$  edge by 14%. These revised data lead to a total oscillator strength consistent with the known electron density and are in agreement with dc-conductivity and stopping-power measurements as well as with absorption coefficients inferred from the cross sections of neighboring elements in the periodic table. The optical functions resulting from this study show evidence for both the redistribution of oscillator strength between energy levels and the effects on real transitions of the shielding of conduction electrons by virtual processes in the core states.

### I. INTRODUCTION

In this paper the problem of constructing a self-consistent set of optical functions for a substance over a wide spectral range is reconsidered. Philipp and Ehrenreich dealt with this question in a classic series of papers.<sup>1,2</sup> However, a reassessment is now timely. The development of synchrotron radiation sources and advances in infrared, x-ray, and electron-energy-loss spectroscopy, as well as improvements in sample preparation, have vastly extended the number and range of reliable measurements. Moreover, advances in the theory have provided new optical sum rules<sup>3-6</sup> by which the self-consistency of optical data can be checked. The latter rules are of particular value as a guide to constructing wide-spectral-range composites, since this requires combining a variety of optical measurements in different energy ranges obtained with various instruments and techniques on different samples.

As an example we consider the optical properties of metallic aluminum. Reasons for this choice are (1) a large volume of experimental data is now available; (2) a number of sets of composite data have been derived,<sup>2,7,8</sup> but contain demonstrable errors<sup>4</sup>; and (3) core excitations in aluminum occur at long enough wavelengths so that corrections<sup>9</sup> to the dipole approximation can be safely ignored and corrections to the attenuation coefficients for Rayleigh, Thomson, and Compton scattering are small relative to the photoelectric effect.<sup>10,11</sup>

Sum-rule tests provide significant guidance in selecting the most probable values from the available optical measurements and in pinpointing systematic errors. For aluminum it has proved possible to generate a comprehensive set of optical functions that not only satisfy all principal sum rules but also are compatible with electron-energy-loss and stopping-power data, provided corrections are made for what appear to be sys-

tematic experimental errors. The principal modification is a reduction of approximately 14% in the reported values of the extinction coefficient in the vicinity of the  $L$  edge. This correction appears to be associated with the presence of surface layers—probably oxides—on the thin-film samples used in the measurements.

A critical review of available experimental data and a full tabulation of our recommended values for the optical constants will be given elsewhere.<sup>12</sup> In the present paper, Sec. II outlines a self-consistent approach to the Kramers-Kronig analysis of experimental data. This is applied to metallic aluminum in Sec. III. The usefulness of electron-energy-loss data in selecting the most reliable optical measurements in the transition region between reflecting and transmitting behavior is discussed in Sec. IV. The use of sum rules as self-consistency tests is discussed in Sec. V, and in Sec. VI the present results are compared with earlier studies.

## II. A SELF-CONSISTENT KRAMERS-KRONIG PROCEDURE FOR METALS

In principle, a Kramers-Kronig dispersion-relation analysis<sup>13</sup> requires the knowledge of one of the optical functions for all frequencies. However, experimentally this requirement is never fulfilled. Thus for metals, experimental optical data<sup>14</sup> commonly involve normal-incidence reflectivity-amplitude measurements or calorimetric-absorbance studies in the infrared, visible, and ultraviolet; critical-angle determinations of the refractive index beyond the plasma frequency (usually in the extreme ultraviolet); and transmission measurements of the absorption coefficient in the extreme ultraviolet and x-ray region. In addition, the angular variation of the reflectance is employed to determine the complex refractive index in the soft-x-ray region. However, these measurements are often at variance with transmission measurements, probably because of surface effects.<sup>15</sup>

Because no one set of measurements covers the entire spectrum, a dispersion-relation analysis is not straightforward. Rather, an iterative procedure must be adopted in which one quantity—e.g., the reflectance—is chosen as a starting point. The chosen quantity is estimated from other optical data in the region in which direct measurements are absent and combined with the directly measured values. Thus one obtains a first approximation to the chosen optical function over the entire wavelength range. The remaining functions may then be calculated and compared with all pertinent measurements. The starting optical function can then be successively modified

until satisfactory agreement is obtained.

This procedure, or at least one cycle of the procedure, has been carried out by Philipp, Ehrenreich, and Segall and Philipp and Ehrenreich<sup>2</sup> for aluminum using the reflectance  $R(\omega)$  as the starting function. Subsequent workers<sup>7,8</sup> repeated this avenue of approach but used the extinction coefficient  $\kappa(\omega)$  as the starting quantity. In principle, there should be no difference in the final result whatever starting function is chosen, provided the calculation is iterated. However, for computational efficiency the choice of the starting function is critical.

If, for a metal,  $\kappa(\omega)$  is chosen as the starting function, it is necessary to derive  $\kappa(\omega)$  values from reflectance data in the far infrared and perhaps in the visible. This may be done by fitting the classic formulas of Drude<sup>16</sup> or of Hagen and Rubens<sup>17</sup> to the infrared reflectance. However, such a procedure often gives a poor initial representation of the data because of the superposition of inter- and intraband transitions in this region.<sup>18,19</sup> The details of the interband structure in the infrared are lost and the resulting values of  $R(\omega)$  are often in poor agreement with experiment.

If, on the other hand, reflectance is chosen as the starting function, experimental values are usually available only below the plasma frequency  $\omega_p$ . However,  $R(\omega)$  values above the plasma frequency can be derived from the measured  $\kappa(\omega)$  values and estimate of  $n(\omega)$  because the normal reflectance is given by<sup>13</sup>

$$R(\omega) = \frac{[n(\omega) - 1]^2 + \kappa^2(\omega)}{[n(\omega) + 1]^2 + \kappa^2(\omega)}. \quad (2.1)$$

Here  $n(\omega)$  and  $\kappa(\omega)$  are the real and imaginary parts of the refractive index. It is possible to estimate  $n(\omega)$  fairly accurately even from an approximate knowledge of the absorption below the plasma frequency. The reason is that the Kramers-Kronig relation<sup>13</sup> for  $n(\omega)$  is linear and can be written as

$$n(\omega) - 1 = \frac{\pi}{2} \text{P} \int_0^{\omega_p} \frac{\omega' \kappa(\omega')}{\omega'^2 - \omega^2} d\omega' + \frac{\pi}{2} \text{P} \int_{\omega_p}^{\infty} \frac{\omega' \kappa(\omega')}{\omega'^2 - \omega^2} d\omega'. \quad (2.2)$$

The second integral on the right-hand side may be evaluated exactly from the measured  $\kappa(\omega)$  values above  $\omega_p$ . Moreover, it is often the major contributor to  $n(\omega) - 1$  for large regions of  $\omega \gg \omega_p$ . For  $\omega \gg \omega_p$  the first integral can be written as

$$-\frac{1}{\omega^2} \int_0^{\omega_p} \omega' \kappa(\omega') \left[ 1 + \left( \frac{\omega'}{\omega} \right)^2 + \dots \right] d\omega'. \quad (2.3)$$

The leading term of this series is  $(1/\omega^2) \int_0^{\omega_p} \omega' \times \kappa(\omega') d\omega'$ , which is proportional to the integrated absorption strength from 0 to  $\omega_p$ . Thus, the contribution to  $n(\omega)$  above  $\omega_p$  from absorptions below  $\omega_p$  is given, to a first approximation, by the total absorption strength below  $\omega_p$ , not by its distribution.

In simple metals such as aluminum the major contribution to the absorption-strength integral  $\int_0^{\omega_p} \omega' \kappa(\omega') d\omega'$  occurs in the visible and ultraviolet, where values of  $\kappa(\omega)$  may be roughly estimated by simple models or are available from ellipsometric measurements. Consequently, reasonably accurate starting values of  $n(\omega)$  for  $\omega > \omega_p$  can be obtained by a Kramers-Kronig transform of a first approximation to the extinction coefficient consisting of (1) measured values above the plasma frequency, (2) values derived from models or ellipsometry in the visible, and (3) approximate values of  $\kappa(\omega)$  in the infrared based on a free-electron-model fit to the reflectivity at the longest wavelengths.

With provisional values of  $\kappa(\omega)$  and  $n(\omega)$  for  $\omega > \omega_p$  in hand, a trial value of the reflectivity above  $\omega_p$  can be calculated from Eq. (2.1) and combined with measured reflectance below  $\omega_p$ . The phase of the reflectivity may then be calculated from the composite reflectance with the Jahoda-Velický dispersion relation.<sup>20,21</sup> The complex refractive index is then given by the inverse Fresnel formula. [See Eqs. (3.2) and (3.3) below.] The iteration then proceeds by using the improved values of  $n(\omega)$  and experimental values of  $\kappa(\omega)$  for  $\omega > \omega_p$  to calculate new values of  $R(\omega)$ , etc.

This procedure assumes the availability of reliable reflectivity measurements characteristic of the bulk material. This is an important proviso since reflectance measurements may be subject to spurious effects resulting from surface conditions such as oxide layers,<sup>22-26</sup> bulk structure,<sup>27,28</sup> and surface roughness which allow coupling to surface plasmons.<sup>29</sup> For aluminum, ultrahigh-vacuum measurements of infrared reflectance<sup>30,31</sup> and smooth-surface reflectance studies in the ultraviolet<sup>32</sup> are available so that the procedure may be carried out. However, as will become apparent, corrections must be made for surface layers in thin-film transmission measurements in the soft-x-ray region.

We have found that by starting with carefully chosen initial values of reflectance a satisfactory fit to most of the experimental data for aluminum may be obtained in one or two full iterations, provided several trial iterations are made to ensure that the optical constants in the region of the bulk plasmons are in agreement with electron-

energy-loss experiments. The full cycle of iterations reproduces the initial data to better than one-half percent.

### III. THE OPTICAL FUNCTIONS OF ALUMINUM

#### A. Initial reflectance data

The initial set of reflectance data for metallic aluminum at room temperature used in this study is shown in Figs. 1 and 2. Below approximately 0.04 eV no reflectance measurements are available and a physically reasonable estimate must be used. We extrapolated the reflectance by use of a free-electron-model fit<sup>33</sup> to the experimental data of Bennett, Silver, and Ashley<sup>30,31</sup> at 0.0517 eV (corresponding to a wavelength of 24  $\mu\text{m}$ ).

From 0.0517 to 11.75 eV direct-reflectance data on evaporated films prepared and measured in vacuum of the order of  $10^{-10}$  torr were employed. These were taken from Bennett *et al.*<sup>30,31</sup> for the region 0.0517–3.00 eV, and from Endriz and Spicer<sup>32</sup> for the region 3.00–11.75 eV. Reflectance values calculated from the ultrahigh-vacuum ellipsometric measurements of Mathewson and Myers<sup>34</sup> in the region 0.7–2.5 eV are in excellent agreement with the measurements of Bennett *et al.*<sup>30</sup> These data were therefore not used as input at this stage. However, the measured pairs of  $n(\omega)$  and  $\kappa(\omega)$  values contain phase in-

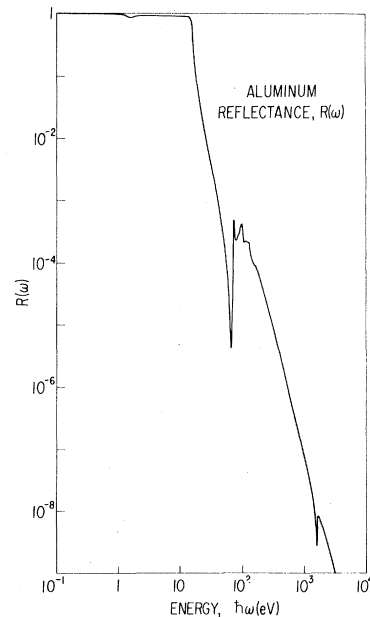


FIG. 1. Reflectance of metallic aluminum at room temperature. Measured reflectance values were employed below the plasma frequency (approximately 15 eV), while above this frequency estimates were based on measured extinction coefficients and trial values of the refractive index obtained by a preliminary Kramers-Kronig analysis. See Sec. II for details.

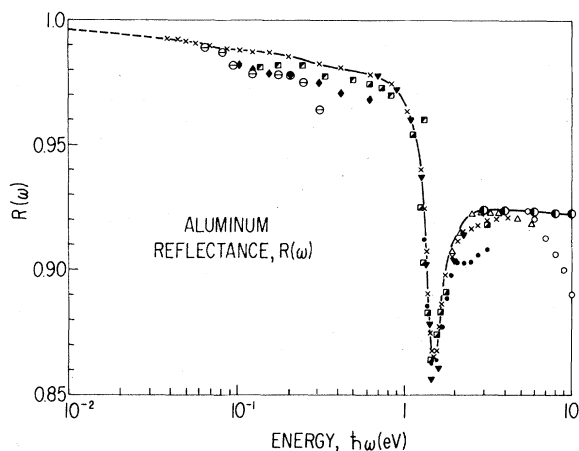


FIG. 2. Reflectance of metallic aluminum at room temperature below the plasma frequency. A free-electron extrapolation was employed below 0.0517 eV. Between 3 and 4 eV the ultrahigh-vacuum measurements of Bennett, Silver, and Ashley (Ref. 30) denoted by  $\times$ , and those of Endriz and Spicer (Ref. 32) denoted by  $\bullet$ , do not coincide; they were joined by a smooth interpolation from 1.66 to 3.0 eV. In making this interpolation the highest reflectance values were chosen as a guide since these are usually associated with the best surfaces. Other data points shown are  $\nabla$ , Mathewson and Myer, Ref. 34;  $\Delta$ , Hass and Waylonis, Ref. 35;  $\circ$ , Schulz, Schulz, and Tangherlini, Ref. 37;  $\square$ , Shklyarevskii and Yarovaya, Ref. 38;  $\circ$ , Daude, Priol, and Robin, Ref. 45;  $\blacklozenge$ , Beattie, Ref. 69;  $\ominus$ , Lenham and Treherne, Ref. 70;  $\blacksquare$ , Golovashkin, Motulevich, and Shubin, Ref. 85.

formation not contained in the reflectance data. This makes the Mathewson and Myers measurements valuable as an independent check on the results of the Kramers-Kronig transformations (see Sec. III C).

The above reflectance data are shown in Fig. 2. In the region of overlap the data of Bennett *et al.* and Endriz and Spicer differ by, at most, 0.6%. The discrepancy is within the limits of error estimated by Bennett *et al.*<sup>30</sup> ( $\pm 0.1\%$ ) and by Endriz and Spicer<sup>32</sup> ( $\sim \pm 0.5\%$ ). However, there is a potentially important qualitative difference. The data of Bennett *et al.* suggest a secondary shoulder between 2.2 and 4.0 eV (which is superimposed on the reflectance dip associated with band-to-band transitions<sup>2,19</sup> near 1.5 eV), while the data of Endriz and Spicer give no hint of this secondary structure.

Other measurements bearing upon this conflict include ultrahigh-vacuum ellipsometric experiments of Mathewson and Myer<sup>34</sup> (0.7–2.5 eV), reflectance studies of Hass and Waylonis<sup>35</sup> on films prepared in conventional vacuums (1.91–5.64 eV) and of Beaglehole as quoted in Ref. 36 (0.6–4.1 eV), as well as measurements of  $n(\omega)$  and  $\kappa(\omega)$  by Schulz and Schulz and Tangherlini<sup>37</sup> and Shklyarev-

skaa and Yarovaya<sup>23,38</sup> employing films deposited in conventional vacuums, absorptivity measurements of Bos and Lynch<sup>39</sup> on polished bulk samples, and thermomodulation studies by Rosei and Lynch<sup>40</sup> on thin-film samples exposed to the atmosphere.

In general the measurements of Schulz *et al.* and of Beaglehole show structure superimposed on the main reflectance dip, while those of Hass and Waylonis and Mathewson *et al.* do not. Of particular importance is the fact that neither the low-temperature data of Bos and Lynch nor the thermoreflectance data of Rosei and Lynch, which should be particularly sensitive, show any secondary structure. Because the weight of evidence is that there is no secondary structure, the smooth interpolation between 1.66 and 3.0 eV shown in Fig. 2 was assumed in the present study. A general policy followed in this interpolation was to choose the highest values of the reflectance in the literature since historically these have been associated with the best surfaces.<sup>24</sup>

The use of data from samples with low surface roughness is essential for energies above several eV because most of the measurements exhibit a sample-dependent surface-plasmon absorption arising from surface roughness.<sup>32,41,42</sup> In aluminum the surface plasmon is located at  $\omega_s = \omega_p / \sqrt{2} \approx 10$  eV, where  $\omega_p$  is the bulk-plasmon frequency.<sup>29</sup> Figure 3 shows this effect. In the present study the uppermost curve was used. It corresponds to the smoothest surface obtained experimentally and appears to be free of surface-plasmon effects. Failure to use smooth-sample data leads to a spurious absorption peak<sup>43</sup> in the bulk-optical functions near the surface-plasmon frequency.

Above 11.8 eV (i.e., above the high-frequency cutoff of the LiF windows employed by Endriz and Spicer), smooth-surface-reflectance data are not yet available so that it was necessary to estimate the reflectance curves from 11.75 to 18 eV. From 11.75 to approximately 15 eV, the bulk-plasmon energy, reflectance measurements on surfaces of unstated roughness yielded lower limits to the estimated values.<sup>44–49</sup> An extremely valuable guide in making these estimates is given by electron-energy-loss spectra. This is discussed in detail in Sec. IV; broadly speaking, the plasmon peak and half width determine the position and steepness of the reflectance falloff, respectively, in the bulk-plasmon region.

A further guide for these estimates is the assumption that at these high energies the joint density of states and matrix elements for optical transitions should be slowly varying. Since the conduction-electron oscillator strength is largely

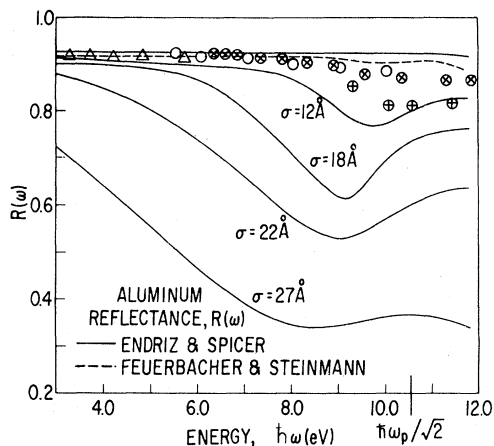


FIG. 3. Reflectance of metallic-aluminum films at room temperature with varying degrees of surface roughness. The solid curves are taken from Endriz and Spicer (Ref. 32) and show increasing absorption by surface plasmons as the rms roughness  $\sigma$  is increased. The uppermost curve is the smoothest obtained experimentally and corresponds to negligible roughness. It is believed to be free of surface-plasmon effects. All other data show these effects to some degree. The dashed curve gives data of Feuerbacher and Steinmann, Ref. 41. Other data points are  $\Delta$ , Hass and Waylonis, Ref. 35;  $\circ$ , Daude, Priol, and Robin, Ref. 45;  $\otimes$ , Madden, Canfield, and Hass, Ref. 48;  $\oplus$ , Vehse, Arakawa, and Stanford, Ref. 47.

exhausted in this range, a more or less featureless monotonic decrease in the extinction coefficient, and in  $\epsilon_2(\omega)$ , is to be expected.<sup>50</sup>

Between 15 and 30 eV, measurements<sup>44,46,48,49</sup> of  $n(\omega)$  and  $\kappa(\omega)$  were employed to calculate the trial reflectance function. From 30 to 4000 eV the values of  $R(\omega)$  calculated by Sasaki and Inokuti<sup>7</sup> were chosen. This set of reflectance data includes the  $L$ - and  $K$ -shell absorption regions. It was obtained by using experimental values<sup>51</sup> of  $\kappa(\omega)$  above  $\omega_p$  and derived values of  $\kappa(\omega)$  below  $\omega_p$ . The latter estimates were largely based on a Drude-model fit in the infrared and ellipsometric studies and model fits in the visible and ultraviolet. In the x-ray range and from 4000 to 10 000 eV the values of Sasaki and Inokuti<sup>7</sup> were supplemented by more recent measurements and by other compilations. These include  $\kappa(\omega)$  values given by Henke and Elgin,<sup>63</sup> Henke and Ebisu,<sup>64</sup> Singman,<sup>65</sup> Lublin *et al.*,<sup>66</sup> Hubbell *et al.*,<sup>67</sup> and the photoelectric cross sections of Davisson.<sup>11</sup> The use of this trial set of reflectance data above 30 eV corresponds to the first step in the iterative procedure described in Sec. II in which an estimate of  $R(\omega)$  is made for  $\omega > \omega_p$ . Free-electron behavior,  $R(\omega) \propto \omega^{-4}$ , was assumed for the high-energy region above 10 000 eV.<sup>68</sup>

### B. Calculation methods

The phase  $\theta$  of the reflection coefficient is given by the Jahoda-Velický dispersion relation<sup>20,21</sup> in its subtracted form<sup>13</sup>

$$\theta(\omega) = -\frac{\omega}{\pi} \int_0^{\infty} \frac{\ln R(\omega') - \ln R(\omega)}{\omega'^2 - \omega^2} d\omega', \quad (3.1)$$

in which the pole at  $\omega' = \omega$  has been removed. Equation (3.1) was evaluated for 506 values of  $\omega$  in the range 0.04 to 10 000 eV. The intervals between these points were chosen smaller in those regions where there is considerable structure, that is, at the location of the band-to-band transitions, i.e., the  $L_{II,III}$  edge, and the  $K$  edge. The trapezoidal rule was used in the numerical integration in the range 0.038 to 11 000 eV. In the low-energy region (below 0.04 eV) and in the high-energy region (above 11 000 eV), the data were represented by analytic fits and were integrated analytically whenever possible. Figure 4 shows the results for  $\theta(\omega)$ .

The refractive index, extinction coefficient, and complex dielectric function were evaluated at these same points from the expressions

$$n(\omega) = \frac{1 - R(\omega)}{1 + R(\omega) - 2\sqrt{R(\omega)} \cos[\theta(\omega)]}, \quad (3.2)$$

$$\kappa(\omega) = \frac{-2\sqrt{R(\omega)} \sin[\theta(\omega)]}{1 + R(\omega) - 2\sqrt{R(\omega)} \cos[\theta(\omega)]}, \quad (3.3)$$

$$\epsilon_1(\omega) = n^2(\omega) - \kappa^2(\omega), \quad (3.4)$$

$$\epsilon_2(\omega) = 2n(\omega)\kappa(\omega), \quad (3.5)$$

where  $\epsilon_1(\omega)$  and  $\epsilon_2(\omega)$  are the real and imaginary parts of the complex dielectric function  $\epsilon(\omega)$ .

In carrying out the iterative calculations a number of determinations<sup>15,59,60</sup> of the optical functions in the soft-x-ray range employing the angular variation of reflectance were not used. The dis-

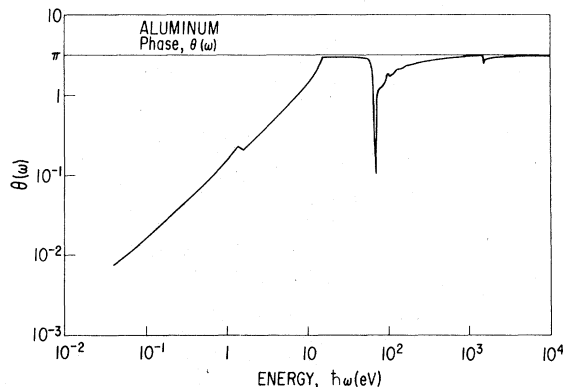


FIG. 4. The phase  $\theta(\omega)$  of the reflectivity of metallic aluminum at room temperature as calculated from the reflectance values of Fig. 1 via Eq. (3.1).

missal is justified because there is considerable disagreement between the absorption coefficient derived from these studies and from direct-transmission measurements.<sup>15</sup> It is speculated that surface roughness or contamination lead to these apparently spurious results; the films employed all appear to have been prepared in conventional vacuums leading to certain oxide contamination, and surface roughness does not seem to have been controlled.

### C. Numerical results

The optical functions resulting from the analysis are shown in graphical form in Figs. 5 and 6; a tabular presentation will be given elsewhere.<sup>12</sup> Values for  $n(\omega)$  are given by the solid curve of Fig. 5; experimental points from ellipsometric, polarimetric, and other measurements are in-

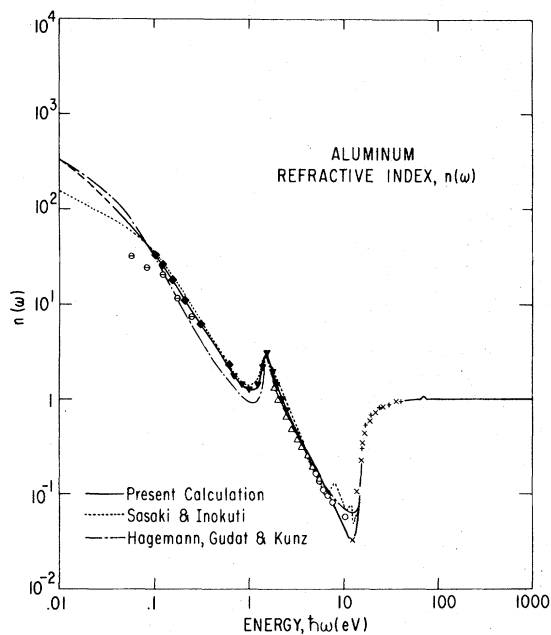


FIG. 5. The refractive index  $n(\omega)$  of metallic aluminum at room temperature. Results of the present study are shown by the solid curve. Independent experimental measurements are given by the data points and recent composites by the broken curves. The structure in the Sasaki-Inokuti results (Ref. 7) near 10 eV is probably attributable to the surface plasmon, as suspected by the authors. Changes in the refractive index arising from the required modification of the absorption data above the  $L$  edge are too small to show on the scale of this graph except near the minimum at 12 eV. Here, for example,  $n(\omega)$  decreased from 0.0353 to 0.0328. Representative data points shown are taken from the work of  $\ominus$ , Lenham and Treherne, Ref. 70;  $\blacklozenge$ , Beattie, Ref. 69;  $\blacktriangledown$ , Mathewson and Myers, Ref. 34;  $\blacktriangle$ , Hass and Waylonis, Ref. 35;  $\circ$ , Daude, Priol, and Robin, Ref. 45;  $\times$ , Ditchburn and Freeman, Ref. 44; and  $+$ , Hunter, Ref. 49.

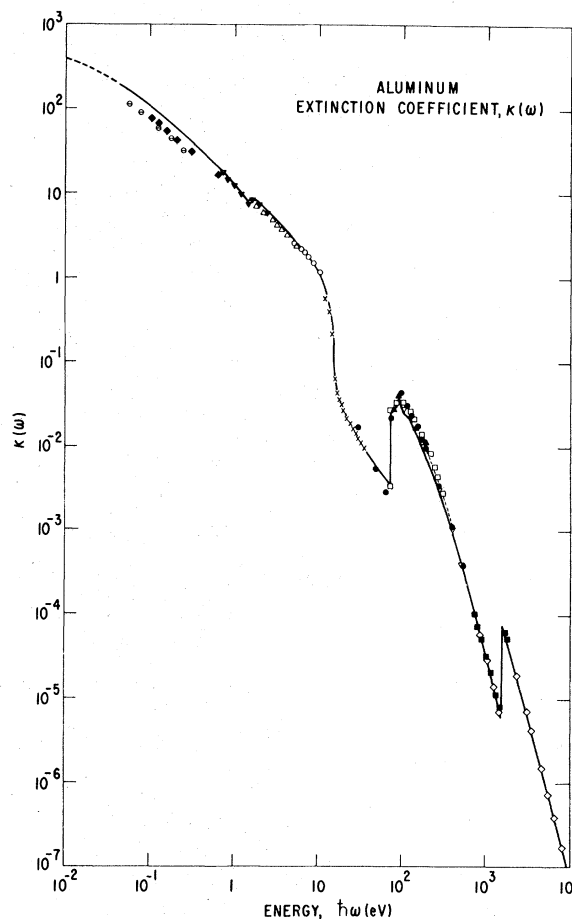


FIG. 6. The extinction coefficient of metallic aluminum. Values derived from the reflectance data of Fig. 1 are shown by the solid curve except just above the  $L$  edge where they are shown by the dashed curve (which accurately passes through the experimental data). Experimental measurements are shown by the data points. Below the plasma frequency (15 eV) the data points and the calculated curve are completely independent. Above the plasma frequency the experimental extinction coefficient forms the basis of the calculation; in this range, agreement between the two indicates freedom from numerical errors. Sum-rule considerations indicate that the experimental data between the  $L$  edge (72.7 eV) and approximately 500 eV are systematically too high. In this range the solid curve gives modified  $\kappa(\omega)$  values which satisfy the  $f$ -sum rule and are in agreement with the most recent measurements of Balzarotti *et al.* (Ref. 96) near the  $L$  edge. Representative data from the following sources are shown:  $\blacklozenge$ , Beattie, Ref. 69;  $\blacktriangle$ , Hass and Waylonis, Ref. 35;  $\blacktriangledown$ , Lukirskii *et al.*, Ref. 15;  $\blacksquare$ , Cook and Stewardson, Ref. 61;  $\blacklozenge$ , Bearden, Ref. 62;  $\times$ , Ditchburn and Freeman, Ref. 44;  $\ominus$ , Lenham and Treherne, Ref. 70;  $\bullet$ , Fomichev and Lukirskii, Ref. 55;  $\circ$ , Daude *et al.*, Ref. 45;  $\square$ , Haensel *et al.*, Ref. 52;  $\blacktriangle$ , Gähwiller and Brown, Ref. 54; and  $\blacktriangledown$ , Mathewson and Myers, Ref. 34.

cluded for comparison. The values of  $n(\omega)$  calculated by Sasaki and Inokuti<sup>7</sup> and by Hagemann, Gudat, and Kunz<sup>8</sup> are also included. The values of Ref. 7 exhibit extraneous structure in the range of 7 to 12 eV, while the values of Ref. 8 do not fit the experimental data well, particularly at lower energies. A comparison of these composites with the present work is given in Sec. VI.

Figure 6 shows the extinction coefficient  $\kappa(\omega)$  calculated from the reflectance data. For comparison, representative experimental measurements are also given. The absorption spectrum consists of an almost-free-electron part at low energies. Superimposed on this is the celebrated interband transition<sup>2,30,37</sup> at approximately 1.5 eV. The interband transition at 0.5 eV, first observed by Bos and Lynch<sup>39</sup> on samples at 4.2 K, is not apparent presumably because of thermal broadening of the absorption peak in the room-temperature data. The  $L$ -shell absorption commences at 72.7 eV and is followed by the  $K$ -shell absorption at 1557 eV.

In comparing the results with experimental points it should be borne in mind that above the plasmon frequency the  $\kappa(\omega)$  values are, in fact, the input data so that the good agreement only signifies that the numerical treatment was accurate. However, below the plasma frequency, the experimental points shown come from direct measurements and are entirely independent of the reflectance data used as input. The agreement with the ultrahigh vacuum ellipsometric measurements of Mathewson and Meyers<sup>34</sup> is particularly good. The most striking disagreement with the refractive index values of Beattie<sup>69</sup> and of Lenham and Treherne<sup>70</sup> probably is attributable to surface contamination of the samples. Similar comments apply to Hodgson's infrared results<sup>71</sup> which are not shown.

#### IV. ELECTRON-ENERGY-LOSS SPECTRA

An independent check on the dielectric function as derived from optical measurements is provided by comparison with electron-energy-loss spectra.<sup>72,73</sup> The differential scattering cross section per unit range of energy loss, per unit solid angle for fast electrons transmitted through a condensed phase, is, in the Born approximation,<sup>74</sup>

$$\frac{d^2\sigma}{d\Omega dE} \propto \frac{1}{q^2} \text{Im} \left( \frac{-1}{\epsilon(\vec{q}, \omega)} \right), \quad (4.1)$$

where  $\epsilon(\vec{q}, \omega)$  is the dielectric function for momentum transfer  $\hbar\vec{q}$  and energy transfer  $E = \hbar\omega$ . It is assumed that the material in question is isotropic or cubic so that  $\epsilon(\vec{q}, \omega)$  is a scalar. The energy-loss measurements extrapolated to  $\vec{q} = 0$  give  $\epsilon(0, \omega)$  values that may be compared di-

rectly with optical data.

In metals the most prominent feature of the energy-loss spectra is a sharp maximum corresponding to the excitation of plasma oscillations in the conduction electrons. These oscillations are associated with the poles in  $1/\epsilon(0, \omega)$  and occur at approximately  $\omega_{p,c}$ , the conduction-electron plasma frequency. This energy also marks the transition between optically transparent and optically reflecting regimes. Here the optical properties change very rapidly and experimental errors may be quite large so that even limited knowledge of the energy-loss function  $\text{Im}[-1/\epsilon(0, \omega)]$  in the plasmon region is valuable for verifying optical measurements.

Electron-energy-loss measurements have been made on aluminum to well beyond the  $L$  edge.<sup>75</sup> Generally the measurements initially yield only relative cross sections; the absolute cross sections derived from them often include large uncertainties. Moreover, the data may be complicated by the superposition of multiple-scattering processes so that reliable values of the energy-loss function are available only near the plasmon frequency. Values of the plasmon peak position  $\omega_p$  and full width at half maximum  $\Delta E_{1/2}$  from several recent studies<sup>76-81</sup> are given in Table I.

The energy-loss function as determined from the best fit to the optical data is given in Fig. 7. Four curves are shown; they correspond to the four possible choices of reflectance spectra shown in Fig. 8. Recall that reliable experimental reflectance measurements on smooth surfaces are available only up to 11.75 eV so that it was necessary to estimate the reflectance from 11.75 to 18 eV. All four estimated curves are consistent with both the smooth-surface-reflectance data below 11.75 eV and with the optical constants determined by interference, critical angle, and other methods above 18 eV. However, only curve d gives an energy-loss function peaking near 15 eV with full width at half maximum of approximately 0.5 eV, the values observed in electron-energy-loss studies.

#### V. TESTS WITH SUM RULES

##### A. Inertial sum rule for $n(\omega)$

We first consider the inertial sum rule,<sup>3,4</sup>

$$\int_0^\infty [n(\omega) - 1] d\omega = 0, \quad (5.1)$$

which states that the average value of the index of refraction is unity. This rule is a direct consequence of causality and the law of inertia; it must be satisfied if  $n(\omega)$  has been calculated from a physically acceptable  $\kappa(\omega)$  by a Kramers-Kronig

TABLE I. Calculated and reported values for the peak energy  $\omega_p$  and full width at half maximum  $\Delta E_{1/2}$  of the bulk plasmon in metallic aluminum. For earlier studies see Kloos, Ref. 79.

Source		$\omega_p$ (eV)	$\Delta E_{1/2}$ (eV)
Calculated present composite		15.0(5)	0.54(5)
Experimental			
Gibbons et al. <sup>a</sup>	(1976)	15.02±0.03	0.54±0.03
Urner-Wille and Raether <sup>b</sup>	(1976)	15.1 ±0.1	
Petri and Otto <sup>c</sup>	(1975)	14.5 ±0.15	
Kloos <sup>d</sup>	(1973)	14.95±0.05	0.5 ±0.05
Zacharias <sup>e</sup>	(1972)	14.95±0.06	0.52±0.05
Geiger and Wittmaack <sup>f</sup>	(1966)	14.97±0.02	0.60±0.02

<sup>a</sup> Reference 76.

<sup>b</sup> Reference 77.

<sup>c</sup> Reference 78.

<sup>d</sup> Reference 79.

<sup>e</sup> Reference 80.

<sup>f</sup> Reference 81.

transform. (For the precise conditions see Ref. 4.) Thus, the rule serves to test the accuracy of the transform procedure as well as the low- and high-energy extrapolations of  $n(\omega)$ . In practice it is convenient to define a verification parameter<sup>4</sup>  $\zeta$  by dividing by the integral of the absolute values of  $n(\omega) - 1$ ,

$$\zeta = \frac{\int_0^\infty [n(\omega) - 1] d\omega}{\int_0^\infty |n(\omega) - 1| d\omega} \quad (5.2)$$

As a result of finite-interval and round-off errors in the numerical procedures, a calculated value of less than 0.005 for  $\zeta$  is considered to indicate good agreement at the level of numerical accuracy em-

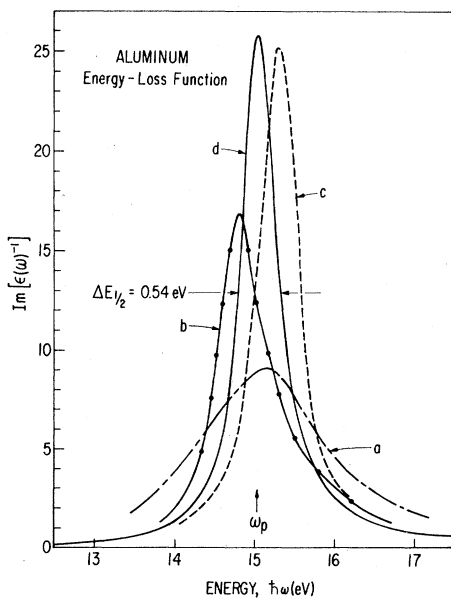


FIG. 7. Calculated electron-energy-loss functions for the various choices of reflectance spectra shown in Fig. 8. Curve d has the experimentally observed peak position,  $\sim 15.0$  eV, and half-width  $\sim 0.5$  eV.

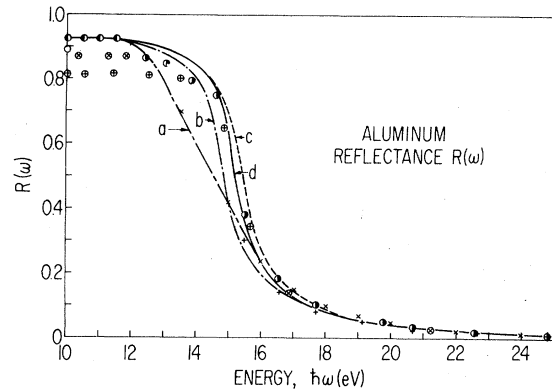


FIG. 8. The reflectance of metallic aluminum in the vicinity of the plasmon frequency. As is apparent from the spread in the data, experimental uncertainty is very high in the region of transition from reflecting to transmitting behavior. Of the four possible interpolations shown, only curve d leads to an electron-energy-loss function with peak position and half-width in agreement with experiment, as seen in Fig. 7. Data points shown are  $\bullet$ , Endriz and Spicer, Ref. 32;  $\times$ , Ditchburn and Freeman, Ref. 44;  $\circ$ , Daude, Priol and Robin, Ref. 45;  $\odot$ , Daude, Savary, Jezequel, and Robin, Ref. 46;  $\oplus$ , Vehse, Arakawa, and Stanford, Ref. 47;  $\otimes$ , Madden, Canfield, and Hass, Ref. 48; and  $+$ , Hunter, Ref. 49.



ployed here.

Using our calculated  $n(\omega)$  for the range 0.04 eV  $< \omega < 10\,000$  eV, the Drude theory for  $\omega \leq 0.04$  eV, and an asymptotic  $\omega^{-2}$  extrapolation for  $n(\omega) - 1$  beyond 10 000 eV, we indeed obtain  $\zeta \approx -0.002$ , i.e., a result indicating satisfactory self-consistency in the present index-of-refraction data. In contrast, Altarelli and Smith<sup>4</sup> obtained from Sasaki and Inokuti's preliminary data<sup>7</sup>  $\zeta = 0.17$ , a result that indicated a large inconsistency in the  $n(\omega)$  calculation. The source of this inconsistency has now been traced to nonanalytic modification of  $n(\omega)$  values in the infrared following the Kramers-Kronig transformation.

#### B. dc-conductivity sum rule

A second consequence of causality and the law of inertia is the sum rule<sup>3</sup>

$$\int_0^{\infty} [\epsilon_1(\omega) - 1] d\omega = -2\pi^2\sigma_0 \quad (5.3)$$

for the dc conductivity  $\sigma_0$ . The only net contribution to this integral is made by the dispersion associated with the conduction electrons. The band-to-band transitions make no net contribution. The rule is, therefore, extremely insensitive to errors in either the magnitude or position of the band-to-band absorptions but provides a test of the conduction-electron spectrum. Equation (5.3) was evaluated using a Drude-theory extrapolation for  $\omega < 0.04$  and the asymptotic  $\omega^{-2}$  behavior of  $\epsilon_1(\omega) - 1$  above 10 000 eV. This yields  $\sigma_0 = 3.21 \times 10^{17} \text{ sec}^{-1}$  (esu) [2.80  $\mu\Omega \text{ cm}$ ]. Representative experimental values for the bulk conductivity at room temperatures are  $3.18 \times 10^{17} \text{ sec}^{-1}$  [2.83  $\mu\Omega \text{ cm}$ ]<sup>82</sup> and  $3.28 \times 10^{17} \text{ sec}^{-1}$  [2.74  $\mu\Omega \text{ cm}$ ].<sup>83</sup> The agreement is good and indicates that the use of a free-electron fit below 0.04 eV is consistent with the higher-energy data and, on the whole, is a sufficiently accurate description of the very-far infrared behavior for present purposes.

This analysis assumes that the evaporated aluminum films employed in measurements of the low-energy portions of the spectrum are representative of the bulk material. This is likely to be the case since rapid deposition rates and ultra-high vacuum were employed.<sup>30</sup> However, it should be pointed out that significantly lower conductivities (i.e., something less than half the bulk values) and attendant differences in optical properties have been reported for thin films formed under other conditions.<sup>84,85</sup>

#### C. The $f$ -sum rule

The  $f$ -sum rule relates the number density of electrons to the dissipative or imaginary parts of

the complex dielectric function, refractive index, and the energy-loss function. It may be written in three distinct forms,<sup>5</sup> i.e.,

$$\int_0^{\infty} \omega' \epsilon_2(\omega') d\omega' = \frac{\pi}{2} \Omega_p^2, \quad (5.4)$$

$$\int_0^{\infty} \omega' \kappa(\omega') d\omega' = \frac{\pi}{4} \Omega_p^2, \quad (5.5)$$

and

$$\int_0^{\infty} \omega' \text{Im}[\epsilon^{-1}(\omega')] d\omega' = -\frac{\pi}{2} \Omega_p^2, \quad (5.6)$$

where  $\Omega_p^2 = 4\pi \mathcal{N}e^2/m$  is the plasma frequency,  $\mathcal{N}$  denoting the total electron density. It is useful to define the effective number of electrons contributing to the optical properties up to an energy  $\omega$  by the partial  $f$  sums:

$$n_{\text{eff}}(\omega)|_{\epsilon} = \frac{m}{2\pi^2 e^2} \int_0^{\omega} \omega' \epsilon_2(\omega') d\omega', \quad (5.7)$$

$$n_{\text{eff}}(\omega)|_{\kappa} = \frac{m}{\pi^2 e^2} \int_0^{\omega} \omega' \kappa(\omega') d\omega', \quad (5.8)$$

$$n_{\text{eff}}(\omega)|_{\epsilon^{-1}} = -\frac{m}{2\pi^2 e^2} \int_0^{\omega} \omega' \text{Im}[\epsilon^{-1}(\omega')] d\omega'. \quad (5.9)$$

In the limit of  $\omega \rightarrow \infty$ , we expect  $n_{\text{eff}}(\infty) = 13$  electrons/atom (hereafter abbreviated as  $e/\text{at.}$ ) for all three rules in aluminum. However, the three partial sums differ significantly as a function of energy, because they describe somewhat different processes.<sup>5</sup>

Figure 9 gives the results for  $n_{\text{eff}}(\omega)$  calculated from the results of the present analysis. A Drude-theory extrapolation was used for  $\omega < 0.04$  eV and a  $\kappa(\omega) \sim \omega^{-4}$  extrapolation<sup>86</sup> for  $\omega > 10\,000$  eV. Below the  $L$  edge the results are shown by the solid curve and above the  $L$  edge by the dashed curve. It is immediately evident that something is wrong: the three forms of  $n_{\text{eff}}(\omega)$  all approach the high-frequency limit of 14.08 rather than 13  $e/\text{at.}$  The fact that all these rules have the same high-frequency limit indicates consistency in the calculation, but the excess oscillator strength implies a fundamental error in the experimental data used as input. Although there is considerable discordance among the input data—some of order  $\pm 10\%$ —this should largely average out in an integral over the entire spectrum so that the excess oscillator strength must result from a systematic error over an important spectral range.

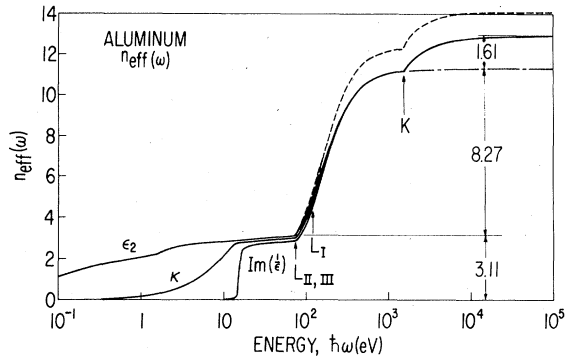


FIG. 9. Values of  $n_{\text{eff}}(\omega)$  for metallic aluminum. The dashed curve shows the results from the reported experimental data and exhibits an unphysical total oscillator strength of over 14  $e/\text{at.}$  rather than 13  $e/\text{at.}$  The solid curve shows  $n_{\text{eff}}(\omega)$  for the modified experimental data in which the extinction coefficient has been reduced by 14% from the  $L$  edge to 300 eV followed by a linearly decreasing percentage reduction from 300 to 500 eV.

A clue to the location of the error is given by partial  $f$  sums over the conduction,  $L$ -shell, and  $K$ -shell absorptions. The partial  $f$ -sum test is possible, because, as is evident in Figs. 6 and 9, absorptions of the various energy levels are widely separated and the oscillator strength of one group of absorptions is almost completely exhausted before the onset of the next.

The principal absorptions of the conduction electrons lie below 15 eV, but the three values of  $n_{\text{eff}}(\omega)$  differ significantly even up to the  $L$  edge at 72.65 eV. This is a result of the polarizable background provided by the  $L$  and  $K$  core states for processes below the  $L$  edge.<sup>5</sup> When the absorptions of the core and conduction electrons are well separated, finite-energy sum rules hold at least approximately for the conduction electrons. These explicitly account for the shielding of the  $f$  sums for  $\kappa(\omega)$  and  $\text{Im}[\epsilon^{-1}(\omega)]$  by the core electrons. The rules have the form<sup>5</sup>

$$\int_0^{\hat{\omega}} \omega' \epsilon_2(\omega') d\omega' \approx \frac{\pi}{2} \omega_{p,c}^2, \quad (5.10)$$

$$\int_0^{\hat{\omega}} \omega' \kappa(\omega') d\omega' \approx \frac{\pi}{4} \frac{\omega_{p,c}^2}{\epsilon_b^{1/2}}, \quad (5.11)$$

$$\int_0^{\hat{\omega}} \omega' \text{Im}\left(\frac{1}{\epsilon(\omega')}\right) d\omega' \approx -\frac{1}{2}\pi (\omega_{p,c}^2/\epsilon_b^2), \quad (5.12)$$

where  $\hat{\omega}$  is an energy at least two to three times the conduction-electron plasmon energy but still below the  $L$  edge. The symbol  $\epsilon_b$  represents the

dielectric function of a fictitious medium consisting of the  $L$ - and  $K$ -shell ion cores alone; the conduction electrons have the plasma frequency  $\omega_{p,c}^2 = 4\pi n_{\text{eff},c} e^2/m$ .

The optical functions derived from the experimental data satisfy these partial sum rules for the conduction electrons to within computational error for  $n_{\text{eff},c} = 3.1(1) e/\text{at.}$  and  $\epsilon_b = 1.04$ .<sup>87</sup> The latter value completely agrees with the dielectric function calculated by a Kramers-Kronig transform of the absorption spectrum of the core electrons alone.

In the region of the  $L$ -shell absorption the  $n_{\text{eff}}(\omega)$  curves draw together as energy increases and are equal to within computational accuracy by the  $K$  edge. Here the "background" dielectric constant arising from the  $K$ -shell polarization is less than 1.0001 so that differences in the three forms of  $n_{\text{eff}}(\epsilon)$  are swamped by roundoff errors in numerical integration.

The effective number of electrons for each group of electrons as calculated from the partial sum rules is given in Table II along with the actual electron occupation. The theoretical oscillator-strength sums of a free atom calculated on the basis of the Hartree-Fock model are given for comparison. The latter values differ from the shell occupation number because of the transfer of oscillator strength between shells.<sup>88,89</sup> According to the Pauli principle, electrons in lower states cannot make transitions to occupied states at higher energies and therefore have oscillator strengths less than they would in the hypothetical case of the single-electron model with no interaction. Similarly, electrons in higher-energy states cannot make downward transitions to occupied core levels and, since such emissions have negative oscillator strengths, this results in an increase in oscillator strength of the higher states.

The magnitude of this redistribution may be estimated easily in the Hartree-Fock approximation. The theoretical values given in Table II are based on dipole matrix elements and energies for aluminum atoms calculated in the Hartree-Fock-Slater (HFS) approximation using atomic-structure programs of Herman and Skillman.<sup>90</sup> These values should also be roughly applicable to metallic aluminum since the core-valence matrix elements and energy differences will be very nearly the same for both atom and metal. In going from the atom to the solid only the valence wave functions are significantly altered. In the region of space important for the matrix elements used in correcting the single-electron model oscillator strength, i.e., where the core wave functions are large, the primary change in the valence-electron

TABLE II. The "effective" number of electrons for the various energy levels in aluminum.

Electronic shell	Atomic parentage	Occupation	"Raw" data	$n_{\text{eff}}(\omega) _c$	
				Modified data	HFS theory
Conduction	$(3s^2, 3p)$	3	3.1(1)	3.1(1)	3.12
L Shell	$(2s^2, 2p^6)$	8	9.3(5)	8.2(7)	8.33
K Shell	$(1s^2)$	2	1.6(1)	1.6(1)	1.55
Total		13	14.0(8)	12.9(9)	13.00

functions is a renormalization. This corresponds to the redistribution of valence-electron charge throughout the atomic volume of the metal and leads to a small correction to the atomic matrix element.<sup>91</sup> Exceptions to all this occur for energies near band edges where the kinetic energy of an excited electron is small and final-state interactions are important. These cause a redistribution of oscillator strength, but little change in the strength when integrated over a wide range.<sup>92</sup> Further, the use of the Hartree-Fock approximation neglects correlation effects, but the atomic Hartree-Fock model should give the correct order of magnitude for the oscillator-strength redistribution.

The experimental value of 3.1(1)  $e/at.$  for the conduction electrons is in good agreement with the theoretical value of 3.1(2)  $e/at.$  Similarly the experimental value<sup>93</sup> of 1.6(1) for the  $K$  shell is in fair agreement with the prediction of 1.5(5). However, the value of 9.3(5) for the  $L$  shell is in disagreement with the Hartree-Fock value of 8.3(3)  $e/at.$  A similar excess oscillator strength in the  $L$ -shell absorption has been observed by Haensel *et al.*<sup>52</sup>

This is in line with the experimental situation: For the three conduction electrons to account for the approximately 1.0(8)  $e/at.$  excess in the total  $f$  sum, there would have to be large error in the infrared and visible spectrum relative to its contribution to  $n_{\text{eff}}$ . This is most unlikely in light of the substantial agreement of the numerous experiments in the region of high conduction-electron absorption. A similar situation holds for the two  $K$ -shell electrons. In contrast, the oscillator strength of the eight  $L$ -shell electrons is largely concentrated between 72 and 500 eV, and a moderate systematic error here could easily account for the excess.

Experiments in the latter energy region involve x-ray transmission studies of thin evaporated films. There are considerable experimental difficulties and the data show a great deal of scatter. In particular, surface effects may not be negli-

ble.<sup>15,59,60</sup> There also appears to be a systematic disagreement between measurements on thin films formed evaporation and those on rolled foils. Measurements for both forms of samples are available only at 525 eV (23.62 Å), where the foil measurements<sup>94,95</sup> yield  $\kappa(\omega)$  values 10% lower than those for thin films.

If the thin-film data are in error and a simple multiplicative correction is applied to the thin-film data, agreement with the  $f$ -sum rule can be obtained by reducing the  $\kappa(\omega)$  values from the  $L$  edge to the neighborhood of 500 eV by 14%. The exact upper limit of the reduced region is not critical for the  $f$  sum. Satisfactory values of both the  $f$  sum and the average excitation energy (as discussed in Sec. VD) are given by a 14% reduction from the  $L$  edge to 300 eV followed by a reduction, varying linearly from 14% at 300 eV to zero at 500 eV. Above 500 eV virtually all measurements have been made on foil samples where bulk effects should be the dominant contributor to the measured values of  $\kappa(\omega)$ . The  $n_{\text{eff}}(\omega)$  values resulting from this *ad hoc* correction are shown in Fig. 9 by the solid curve and the contribution of the various shells is given in Table II, col. 5. Using the reduced absorption between 72.65 and 500 eV leads to a total  $n_{\text{eff}}(\omega)$  contribution for the  $L$ -shell electrons of 8.2(7), which is in good agreement with the HFS theory value of 8.3(3).

Recent work by Balzarotti *et al.*<sup>96,97</sup> provides good evidence for the validity of our correction near the  $L$  edge. By using films of various thickness these authors have separated surface and bulk effects. Although their published data<sup>96</sup> extend only 10 eV above the  $L$  edge, their  $\kappa(\omega)$  values are consistently some 15% below the values of Haensel *et al.*,<sup>52,53</sup> Gähwiller and Brown,<sup>54</sup> Fomichev *et al.*,<sup>55-57</sup> and Lukirskii *et al.*<sup>15</sup> used in preparing the original input data.

Further evidence for this systematic overestimate of  $\kappa(\omega)$  in most thin-film data is the extremely close agreement between the revised values found here and the semiempirical photoelectric cross sections given by Henke and Elgin<sup>63</sup>

in the range 150 to 500 eV. The latter cross sections are polynomial "best-fit" parametrization of atomic data based on cross-section measurements of a variety of light elements so that systematic errors associated with a particular element are reduced. (In general, these fits give only average behavior in the region above an absorption edge where chemical bonding and other effects yield structure so that a detailed comparison below 150 eV has little meaning.)

A possible explanation of the apparent experimental error is the presence of an oxide layer at the surface. It has been established that a layer of oxide ranging from 20–50 Å in terminal thickness quickly grows on a clean aluminum surface exposed to air.<sup>22,26,98</sup> All thin-film samples employed in the absorption studies were prepared by evaporation, but at relatively modest vacuums (at best  $10^{-6}$  torr), and subsequently exposed to air; oxide films were certainly present and in some instances oxygen may have been included in the film during growth. Moreover, many of the experiments used unbacked films formed either on alkali-halide or organic-film substrates, which were subsequently dissolved away. This additional operation admits the possibility of forming thicker or more complex surface layers.

Possible effects of surface layers are redistribution of absorption strength near x-ray edges and the introduction of errors in interferometric thickness measurements. The first arises from potential-barrier effects, which are known in molecules as well as solids.<sup>92</sup> It is most pronounced in thin films with large surface-layer to bulk volume ratios. Although there is no change in the total oscillator strength for a given film, combining data from films of different thickness could give erroneous  $f$  sums. The second effect arises from altered phase shifts<sup>99(a)</sup> at the vacuum-surface-layer-aluminum interface. An experimental test of the importance of these effects would be optical and interferometric studies of films with controlled degrees of exposure to the atmosphere.

A further complication which should be noted is that evaporated films frequently have lower density than the bulk form of the same material.<sup>99(b)</sup> The effect of this circumstance on calculated atomic absorption cross sections depends on how the atomic density per unit area of the film is determined. If it is found from a mass measurement—say, by using a vibrating-crystal monitor—there is no error, in principle. However, if the thickness is measured by interferometry and the bulk density simply assumed, the resulting absorption coefficient comes out too low if the film density is less than that of the bulk. This is the opposite of what is observed here. In the experi-

mental measurements on aluminum near the  $L_{II,III}$  edge both methods have been employed so that a variation in density does not seem sufficient to explain the "observed" excess absorption.

The revision of the  $L$ -shell absorption data leads to a small decrease in the background dielectric function  $\epsilon_b$ , as calculated by Eqs. (5.10)–(5.12). This averages 0.005, yielding a revised value of  $\epsilon_b = 1.03(5)$ . Since the conduction-electron absorption is unaffected by the correction, there is no change in  $\sigma_0$  as calculated by Eq. (5.3) in Sec. V B.

#### D. Mean excitation energy for stopping power

The dielectric response function governs the energy loss of fast charged particles penetrating through matter, as we have seen in the electron-energy-loss measurements. As a consequence the mean energy loss per unit pathlength, i.e., the stopping power, depends upon an integral of the response function. The basic theory was originally established by Bethe<sup>100</sup> and worked out more generally by Fano<sup>101,102</sup> and others. In the well-known expression for the stopping power [Eq. (38) of Fano<sup>102</sup>], there appears the mean excitation energy  $I$  defined by

$$\ln I = \frac{\int_0^\infty \omega \ln \omega \operatorname{Im}[\epsilon^{-1}(\omega)] d\omega}{\int_0^\infty \omega \operatorname{Im}[\epsilon^{-1}(\omega)] d\omega}. \quad (5.13)$$

Indeed,  $I$  is the only quantity that depends on electronic structure of the material. In other words,  $I$  embodies the material property pertinent to glancing collisions of the incident particle; hard collisions, in contrast, contribute to stopping power an amount roughly independent of the electronic structure.

The evaluation of  $I$  from a knowledge of the response function (which in essence amounts to the oscillator-strength distribution, for free atoms and molecules) has been carried out for many instances, as recently reviewed by Inokuti and Turner.<sup>103</sup> Experimentally,  $I$  is deduced from analysis of the energy dependence of the stopping power.

As may be seen from Eq. (5.13), the average excitation energy is most sensitive to the higher-energy portions of the spectrum. This is indicated in Fig. 10, which shows the cumulative value of  $I$  for aluminum as a function of the upper limit of integration in Eq. (5.13). The three conduction electrons account for 23% of the electron density, but make only a 10% contribution to  $I$ . Thus the mean excitation energy serves as a test of the  $L$ - and  $K$ -shell spectra, particularly their higher-energy portions.

This situation was exploited in determining the

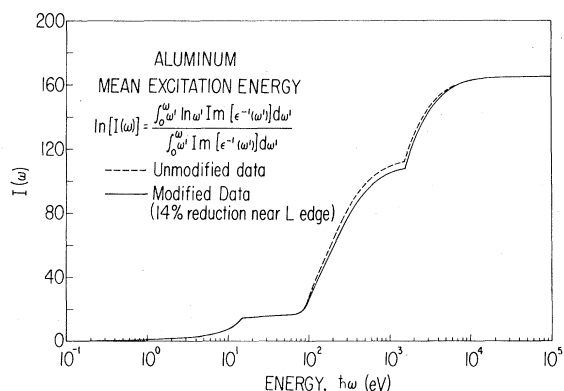


FIG. 10. The average excitation energy  $I$  as defined by Eq. (5.13) as a function of the upper limit of integration. The solid curve shows  $I$  for the optical functions as modified above the  $L$  edge, while the dashed curve applies to the unmodified values derived from the reported data.

energy interval over which the  $L$ -shell absorption should be modified to ensure that the total  $f$  sum equaled  $13 e/at$ . By simultaneously requiring that both the  $f$ -sum rule be satisfied and that the mean excitation energy agree with experiment, it was found that the best agreement was obtained for a 14% reduction of the reported  $\kappa(\omega)$  values from the  $L$  edge to 300 eV followed by a smoothly varying reduction decreasing linearly from 14% at 300 eV to zero at 500 eV. Although any such integral constraint can provide only general guidance, it is significant in cases such as this where the region of experimental uncertainty can be isolated by other considerations such as the partial  $f$  sums. For example, a modification consisting of a 13.5% reduction in  $\kappa(\omega)$  from the  $L$  edge to 400 eV followed by a smoothly varying reduction decreasing linearly from 13.5% at 400 eV to zero at 700 eV yields an  $f$  sum of  $13 e/at$ , but a mean excitation energy several eV lower than the modification described above.

Values of  $I$  calculated with and without the 14% modifications in the  $L$ -shell absorption are shown in Table III, together with an early theoretical determination based on the atomic oscillator-strength distribution<sup>104</sup> and various experimental values.<sup>105-107</sup> Uncertainties in the calculated values of  $I$  associated with extrapolations of  $\kappa(\omega)$  to energies greater than 10 000 eV are estimated<sup>108</sup> to be less than  $\pm 1 eV$ . The most accurate experimental value is thought to be 167 eV by Bichsel and co-workers.<sup>105,107</sup> Uncertainties in the experimental value arise from the shell corrections and other terms in the stopping power, as well as from uncertainties in the measurements. These uncertainties appear to be of the order of a few eV when translated into  $I$ .

## VI. COMPARISON WITH OTHER COMPOSITES

### A. Early work

The present results and those of Philipp and Ehrenreich's 1964 study<sup>2</sup> are in qualitative agreement, but differ in detail because of the newer data used here. In general Philipp and Ehrenreich's results show a deficiency in oscillator strength at high energies as a consequence of early x-ray absorption measurements which gave systematically too small extinction coefficients above the  $L_{II,III}$  edge. Extraneous effects resulting from surface-plasmon absorption are also apparent in their work in the neighborhood of 10 eV.

### B. Sasaki and Inokuti's 1971 composite<sup>7</sup>

The initial impetus for the present research was the discovery<sup>4</sup> that the inertial sum rule was not satisfied by Sasaki and Inokuti's  $n(\omega)$  values. At the time the reason was conjectured to be values which were too small below 0.1 eV; this is substantiated by the present calculation. In the work of Sasaki and Inokuti,  $n(\omega)$  values were first calculated by a Kramers-Kronig transform from  $\kappa(\omega)$  but were *subsequently* modified by a non-

TABLE III. Mean excitation energy  $I$  for metallic aluminum.

Source	$I$ (eV)
Calculated	
Present work: A. Unmodified $\epsilon(\omega)$ data	165.6(7)
B. Modified $\epsilon(\omega)$ data	165.7(1)
Atomic oscillator strength (theory) <sup>a</sup>	124
Experimental	
Bichsel and Uehling <sup>b</sup> (1960), Turner <i>et al.</i> <sup>c</sup> (1970)	163
Tschalär and Bichsel <sup>d</sup>	167

<sup>a</sup> Reference 104.

<sup>b</sup> Reference 105.

<sup>c</sup> Reference 106.

<sup>d</sup> Reference 107.

analytic procedure. The modification was made to bring the calculated values of  $n(\omega)$  and  $\kappa(\omega)$  into agreement with reflectivity measurements below 0.1 eV. However, the procedure employed a Hagen-Rubens extrapolation in the infrared, a region which is particularly complicated because of the simultaneous presence of free-electron and band-to-band processes.

A second major difference is the structure present in Sasaki and Inokuti's  $n(\omega)$  values between 6 and 12 eV. This structure is almost certainly spurious, as already suspected by these authors. It is partially associated with small undulations in the  $\kappa(\omega)$  values used as input between 5 and 10 eV. These  $\kappa(\omega)$  values were obtained from polarimetric experiments and the angular variation of reflectance. They were subsequently modified to obtain agreement with reflectance measurements of Feuerbacher and Steinmann.<sup>41</sup> The latter reflectance data show a small drop arising from surface roughness so that the structure in  $n(\omega)$  near 10 eV is most probably attributable to residual surface-plasmon absorption. There is also the possibility that it is an absorption associated with a surface plasmon shifted in energy by the presence of a surface layer.<sup>109</sup>

In addition, Sasaki and Inokuti encountered a persistent problem of oscillator strengths in excess of 13  $e/at$ . Attempts to eliminate this by favoring experiments yielding lower  $\kappa(\omega)$  values were never completely successful. The difficulty is the same as encountered in the present work, viz., systematically high values of the absorption coefficient above the  $L_{II,III}$  edge probably as a result of surface effects (discussed in Sec. VC).

#### C. Hagemann, Gudat, and Kunz's 1974 composite

Hagemann, Gudat, and Kunz<sup>8</sup> (HGK) chose  $\kappa(\omega)$  as the starting point for their study, but relied on a free-electron model at low energies and did not iterate the calculation to obtain self-consistency with reflectance data. The HGK results for  $\kappa(\omega)$  are very similar to the unmodified  $\kappa(\omega)$  values of the present study except below approximately 0.1 eV; here the HGK values exceed the present ones by 10 to 20%.

This additional absorption is reflected in  $n(\omega)$  as a dispersion-like deviation from the present results: Below 0.08 eV the HGK values for  $n(\omega)$  exceed the present one while they are less than the present values by a factor of  $\frac{2}{3}$  over most of the region from 0.08 to 1.5 eV. This is in significant disagreement with direct measurements of  $n(\omega)$ .

Application of the  $f$ -sum rule to the HGK data indicates two problems: excess oscillator strength in the x-ray region and inconsistencies at low energies, probably in the infrared. The complete

$f$  sums from 0 to  $\infty$  for  $\epsilon_2$ ,  $\kappa$ , and  $\text{Im}\epsilon^{-1}$  are 13.4, 13.6, and 13.6  $e/at$ , respectively. The oscillator strength in excess of 13  $e/at$  is almost certainly a result of systematic errors in the  $L$ -shell spectrum similar to those encountered in the present work. The differences in magnitude of the  $f$  sum for  $\epsilon_2$ ,  $\kappa$ , and  $\text{Im}\epsilon^{-1}$  indicate an inconsistency or numerical inaccuracies. It is equivalent to a failure of the Stern sum rule.<sup>3,13,110</sup> The probable origin can be traced with a plot of the various partial  $f$  sums (see Fig. 35 of the second citation in Ref. 8). It is found that  $n_{\text{eff}}(\omega)|_{\epsilon_2}$  crosses  $n_{\text{eff}}(\omega)|_{\kappa}$  at approximately 10 eV and remains below  $n_{\text{eff}}(\omega)|_{\kappa}$  up to the  $L_{II,III}$  edge. From Eqs. (5.10)–(5.12) this implies a background dielectric function less than unity, i.e., a negative polarizability of the ion cores below their absorption edges. This is, of course, impossible, showing that an inconsistency between  $\epsilon_2(\omega)$  and  $\kappa(\omega)$  lies below 10 eV. Furthermore, all values of  $n_{\text{eff}}(\omega)$  are less than three below the  $L_{II,III}$  edge. This is most unlikely because the oscillator strength of the three conduction electrons is virtually exhausted below the  $L_{II,III}$  edge.

The discrepancies at low energies and perhaps some of the partial  $f$ -sum-rule inconsistencies can be attributed to the use in the range 0.001 to 0.8 eV of  $\kappa(\omega)$  values from a Drude-model fit based on the dc conductivity and plasma frequency. Although this reproduces the reflectance from 0.05 to 0.15 eV reasonably accurately, it unnecessarily constrains the optical functions. In fact, the HGK values of  $n(\omega)$  do not reproduce those of the original free-electron model used as input in this range. A similar situation holds for the reflectance. The reason is almost certainly the presence of a superposition of inter- and intra-band transitions and the background polarization of the ion cores. The use of a free-electron model imposes a particular relation between  $n(\omega)$  and  $\kappa(\omega)$ , which is inconsistent with interband processes. It can be used only for energies where interband absorptions are dominant (less than about 0.1 eV in the present case).

#### D. Conclusions

The major discrepancies between recent composites and the present study are in the infrared, the ultraviolet, and above the  $L$  edge. The first arises from the inappropriateness of free-electron-model fits to reflectance to obtain  $\kappa(\omega)$  for use as input values at low energies where band-to-band transitions are also important. The second is due to a surface-plasmon component in reflectance data on samples with rough surfaces. The third arises from what appears to be a systematic error in most thin-film x-ray-absorption

studies.

This study has thus brought into question a number of optical measurements on aluminum and has pinpointed regions of the spectrum where more precise experiments are needed. Especially critical are the regions from the  $L$  edge to 500 eV and in the vicinity of the plasmon resonance. In the former, uncertainties associated with surface layers should be eliminated. In the latter, reflectance and ellipsometric studies are needed for smooth samples in ultrahigh vacuum beyond the cutoff of LiF windows.

#### ACKNOWLEDGMENTS

The authors would like to acknowledge the aid and counsel of numerous colleagues during the course of this research. Particular thanks are due to Professor F. C. Brown and Dr. E. M. Pell for discussions concerning experimental procedures and difficulties in the soft-x-ray region, and Professor P. C. Gibbons for providing his unpublished electron-energy-loss data. The work was performed under the auspices of the U.S. Department of Energy.

\*Present address: Mailstop 21, ECAC, IIT Research Institute, Annapolis, Maryland 21402.

- <sup>1</sup>See, for example, H. Ehrenreich and H. R. Philipp, *Phys. Rev.* **128**, 1622 (1962); H. R. Philipp and H. Ehrenreich, *ibid.* **129**, 1550 (1963); **131**, 2016 (1963).
- <sup>2</sup>H. R. Philipp and H. Ehrenreich, *J. Appl. Phys.* **35**, 1416 (1964). See also Ref. 50.
- <sup>3</sup>M. Altarelli, D. L. Dexter, H. M. Nussenzveig, and D. Y. Smith, *Phys. Rev. B* **6**, 4502 (1972).
- <sup>4</sup>M. Altarelli and D. Y. Smith, *Phys. Rev. B* **9**, 1290 (1974).
- <sup>5</sup>D. Y. Smith and E. Shiles, *Phys. Rev. B* **17**, 4689 (1978).
- <sup>6</sup>W. M. Saslow, *Phys. Lett.* **33A**, 157 (1970); A. Villani and A. H. Zimerman, *Phys. Rev. B* **8**, 3914 (1973) and *Phys. Lett.* **44A**, 295 (1973); K. Furuya, A. H. Zimerman, and A. Villani, *Phys. Rev. B* **13**, 1357 (1976); F. W. King, *J. Math. Phys.* **17**, 1509 (1976).
- <sup>7</sup>T. Sasaki and M. Inokuti, *Conference Digest of the Third International Conference on Vacuum Ultraviolet Radiation Physics*, edited by Y. Nakai (*Phys. Soc. of Jpn.*, Tokyo, 1971), p. 2aC2-2. See, also, Argonne National Laboratory Report ANL-7860, Pt. I, p. 47, 1971 (unpublished).
- <sup>8</sup>H.-J. Hagemann, W. Gudat, and C. Kunz, *J. Opt. Soc. Am.* **65**, 742 (1975), and DESY Report SR 74/7, Hamburg, 1974 (unpublished).
- <sup>9</sup>L. I. Schiff, *Quantum Mechanics*, 3rd ed. (McGraw-Hill, New York, 1968).
- <sup>10</sup>For example, for aluminum at 10 keV, the photoelectric attenuation coefficient for coherent (Rayleigh and Thomson) scattering is 20.7 b/atom and that for incoherent (Compton) scattering is 8.3 b/atom compared with a photoelectric cross section of 1145 b/atom. See Ref. 11, Appendix I.
- <sup>11</sup>C. M. Davisson, *Interaction of  $\gamma$ -Radiation with Matter in Alpha-, Beta-, and Gamma-Ray Spectroscopy*, edited by K. Siegbahn (North-Holland, Amsterdam, 1965), Vol. I, p. 37.
- <sup>12</sup>E. Shiles and D. Y. Smith (unpublished).
- <sup>13</sup>See, for example, F. Stern, in *Solid State Physics*, edited by F. Seitz and D. Turnbull (Academic, New York, 1963), Vol. 15, p. 300.
- <sup>14</sup>For a brief review of experimental methods and further references, see M. P. Givens, in *Solid State Physics*, edited by F. Seitz and D. Turnbull (Academic, New York, 1958), Vol. 6, p. 313.
- <sup>15</sup>A. P. Lukirskii, E. P. Savinov, O. A. Ershov, and Yu. F. Shepelev, *Opt. Spektrosk.* **16**, 310 (1964) [*Opt. Spectrosc.* **16**, 168 (1964)].
- <sup>16</sup>P. Drude, *Lehrbuch der Optik*, 2nd ed. (S. Hirzel, Leipzig, 1906) [*Theory of Optics* (Longmans-Green, New York, 1920)].
- <sup>17</sup>E. Hagen and H. Rubens, *Ann. Phys. (Leipzig)* **11** (4), 873 (1903).
- <sup>18</sup>C. J. Powell, *J. Opt. Soc. Am.* **60**, 78 (1970).
- <sup>19</sup>D. Brust, *Phys. Rev. B* **2**, 818 (1970).
- <sup>20</sup>F. C. Jahoda, thesis, Cornell University, 1957 (unpublished); B. Velický, *Czech. J. Phys. B* **11**, 541 (1961).
- <sup>21</sup>D. Y. Smith, *J. Opt. Soc. Am.* **67**, 570 (1977).
- <sup>22</sup>P. H. Berning, G. Hass, and R. P. Madden, *J. Opt. Soc. Am.* **50**, 586 (1960).
- <sup>23</sup>I. N. Shklyarevskii and R. G. Yarovaya, *Opt. Spektrosk.* **14**, 252 (1963) [*Opt. Spectrosc.* **14**, 130 (1963)].
- <sup>24</sup>R. W. Fane and W. E. J. Neal, *J. Opt. Soc. Am.* **60**, 790 (1970).
- <sup>25</sup>J. Shewchun and E. C. Rowe, *J. Appl. Phys.* **41**, 4128 (1970).
- <sup>26</sup>J. H. Halford, F. K. Chin, and J. E. Norman, *J. Opt. Soc. Am.* **63**, 786 (1973).
- <sup>27</sup>W. E. J. Neal, R. W. Fane, and N. W. Grimes, *Philos. Mag.* **21**, 167 (1970).
- <sup>28</sup>G. P. Motulevich, A. A. Shubin, and O. F. Shustova, *Zh. Eksp. Teor. Fiz.* **49**, 1431 (1965) [*Sov. Phys.—JETP* **22**, 984 (1966)].
- <sup>29</sup>R. H. Ritchie, *Phys. Rev.* **106**, 874 (1957).
- <sup>30</sup>H. E. Bennett, M. Silver, and E. J. Ashley, *J. Opt. Soc. Am.* **53**, 1089 (1963).
- <sup>31</sup>H. E. Bennett and J. M. Bennett, in *Optical Properties and Electronic Structure of Metals and Alloys*, edited by F. Abelès (North-Holland, Amsterdam, 1966), p. 175.
- <sup>32</sup>J. G. Endriz and W. E. Spicer, *Phys. Rev. B* **4**, 4144 (1971); **4**, 4159 (1971).
- <sup>33</sup>A free-electron-model fit ignores corrections for effects such as exchange and Coulomb correlation, non-locality, etc. [See, for example, P. Vashishta and K. S. Singwi, *Phys. Rev. B* **6**, 875 (1972)], complications of the normal and anomalous skin effects [for a review see, G. P. Motulevich, in *Proceedings (Trudy) of the P. N. Lebedev Physics Institute*, edited by D. V. Skobel'tsyn (Consultants Bureau, New York, 1973),

Vol. 55]. However, for present purposes, all that is required is a physically reasonable analytic continuation of  $R(\omega)$  to zero frequency, and experimentation with a number of fits shows that the derived optical constants and the sum-rule integrals are relatively insensitive to the low-energy extrapolation in the present example, where data are available well into the infrared.

From 0.0517 to 0.124 eV (24 to 10  $\mu\text{m}$ ) the reflectance data of Bennett, Silver, and Ashley can be fit with reasonable accuracy to a free-electron model (see Ref. 31). This is in agreement with Brust's calculations (Ref. 19), which show that interband effects should be small relative to intraband effects at these energies.

Below 0.0517 eV (24  $\mu\text{m}$ ) the reflectance data rise somewhat faster with wavelength than predicted by this fit. The effect is small [ $\approx 0.002\%$  in  $R(\omega)$ ] and involves only the last four data points extending to 0.039 eV (32  $\mu\text{m}$ ). A better fit is given if two classes of free electrons are employed (see Ref. 18), but for present purposes assumption of a simple free-electron behavior below 0.05 eV appears adequate. The  $n(\omega)$  and  $\kappa(\omega)$  values resulting from the Kramers-Kronig transformation of the reflectance reproduce the input data to better than 0.5% throughout the entire infrared region and the dc conductivity given by the Drude extrapolation is equal to the experimental value within experimental error.

- <sup>34</sup>A. G. Mathewson and H. P. Myers, *Phys. Scr.* **4**, 291 (1971).
- <sup>35</sup>G. Hass and J. E. Waylonis, *J. Opt. Soc. Am.* **51**, 719 (1961).
- <sup>36</sup>G. Dresselhaus, M. S. Dresselhaus and D. Beaglehole, in *Electronic Density of States*, edited by L. H. Bennett, NBS Special Publication 323 (National Bureau of Standards, Washington, D. C., 1971).
- <sup>37</sup>L. G. Schulz, *J. Opt. Soc. Am.* **44**, 357 (1954), and L. G. Schulz and F. R. Tangherlini, *ibid.* **362** (1954).
- <sup>38</sup>I. N. Shklyarevskii and R. G. Yarovaya, *Opt. Spektrosk.* **16**, 85 (1964) [*Opt. Spectros.* **16**, 45 (1964)].
- <sup>39</sup>L. W. Bos and D. W. Lynch, *Phys. Rev. Lett.* **25**, 156 (1970).
- <sup>40</sup>R. Rosei and D. W. Lynch, *Phys. Rev. B* **5**, 3883 (1972).
- <sup>41</sup>B. P. Feuerbacher and W. Steinmann, *Opt. Commun.* **1**, 81 (1969).
- <sup>42</sup>A. Daude, A. Savary, and S. Robin, *Thin Solid Films* **13**, 255 (1972).
- <sup>43</sup>M. W. Williams, E. T. Arakawa, and L. C. Emerson, *Surf. Sci.* **6**, 127 (1967).
- <sup>44</sup>R. W. Ditchburn and G. H. C. Freeman, *Proc. R. Soc. London, Ser. A* **294**, 20 (1966).
- <sup>45</sup>A. Daude, M. Priol, and S. Robin, *C. R. Acad. Sci. (Paris) B* **263**, 1178 (1966).
- <sup>46</sup>A. Daude, A. Savary, G. Jezequel, and S. Robin, *C. R. Acad. Sci. (Paris) B* **269**, 901 (1969).
- <sup>47</sup>R. C. Vehse, E. T. Arakawa, and J. L. Stanford, *J. Opt. Soc. Am.* **57**, 551 (1967).
- <sup>48</sup>R. P. Madden, L. R. Canfield, and G. Hass, *J. Opt. Soc. Am.* **53**, 620 (1963).
- <sup>49</sup>W. R. Hunter, *J. Opt. Soc. Am.* **54**, 208 (1964) and *J. Phys. (Paris)* **25**, 154 (1964); see also, *Opt. Acta* **9**, 255 (1962) and *J. Appl. Phys.* **34**, 1565 (1963).
- <sup>50</sup>H. Ehrenreich, H. R. Philipp, and B. Segall, *Phys. Rev.* **132**, 1918 (1963).

- <sup>51</sup>The optical functions prepared by Sasaki and Inokuti are a composite of the data of Lukirskii *et al.*, Ref. 15; Bennett, Silver, and Ashley, Ref. 30; Hass and Waylonis, Ref. 35; Feuerbacher and Steinmann, Ref. 41; Ditchburn and Freeman, Ref. 44; Daude, Savary, Jezequel, and Robin, Ref. 46; Vehse, Arakawa, and Stanford, Ref. 47; Madden, Canfield, and Hass, Ref. 48; Hunter, Ref. 49; Haensel *et al.*, Refs. 52 and 53; Gähwiller and Brown, Ref. 54; Fomichev *et al.*, Refs. 55, 56, and 57; Singer, Ref. 58; Ershov *et al.*, Refs. 59 and 60; Cooke and Stewardson, Ref. 61, and Bearden, Ref. 62.
- <sup>52</sup>R. Haensel, B. Sonntag, C. Kunz, and T. Sasaki, *J. Appl. Phys.* **40**, 3046 (1969).
- <sup>53</sup>R. Haensel, G. Keitel, B. Sonntag, C. Kunz, and P. Schreiber, *Phys. Status Solidi A* **2**, 85 (1970).
- <sup>54</sup>C. Gähwiller and F. C. Brown, *Phys. Rev. B* **2**, 1918 (1970).
- <sup>55</sup>V. A. Fomichev and A. P. Lukirskii, *Opt. Spektrosk.* **22**, 796 (1967) [*Opt. Spectrosc.* **22**, 432 (1967)].
- <sup>56</sup>V. A. Fomichev and A. P. Lukirskii, *Fiz. Tverd. Tela.* **8**, 2104 (1966) [*Sov. Phys.-Solid State* **8**, 1674 (1967)].
- <sup>57</sup>V. A. Fomichev, *Fiz. Tverd. Tela* **8**, 2892 (1966) [*Sov. Phys.-Solid State* **8**, 2312 (1967)].
- <sup>58</sup>S. Singer, *J. Appl. Phys.* **38**, 2897 (1967).
- <sup>59</sup>O. A. Ershov, I. A. Brytov, and A. P. Lukirskii, *Opt. Spektrosk.* **22**, 127 (1967) [*Opt. Spectrosc.* **22**, 66 (1967)].
- <sup>60</sup>O. A. Ershov and I. A. Brytov, *Opt. Spektrosk.* **22**, 305 (1967) [*Opt. Spectrosc.* **22**, 165 (1967)].
- <sup>61</sup>B. A. Cooke and E. A. Stewardson, *Br. J. Appl. Phys.* **15**, 1315 (1964).
- <sup>62</sup>A. J. Bearden, *J. Appl. Phys.* **37**, 1681 (1966).
- <sup>63</sup>B. L. Henke and R. L. Elgin, in *Advances in X-Ray Analysis*, edited by B. L. Henke, J. B. Newkirk, and G. R. Mallett (Plenum, New York, 1970), Vol. 13, p. 639.
- <sup>64</sup>B. L. Henke and E. S. Ebusu, in *Advances in X-Ray Analysis*, edited by C. L. Grant, C. S. Barrett, J. B. Newkirk, and C. O. Ruud (Plenum, New York, 1974), Vol. 17, p. 150.
- <sup>65</sup>L. Singman, *J. Appl. Phys.* **45**, 1885 (1974).
- <sup>66</sup>P. Lublin, P. Cukor, and R. J. Jaworowski, in *Advances in X-Ray Analysis*, edited by B. L. Henke, J. B. Newkirk, and G. R. Mallett (Plenum, New York, 1970), Vol. 13, p. 632.
- <sup>67</sup>J. H. Hubbell, W. H. McMaster, N. K. Del Grande, and J. H. Mallett, in *International Tables for X-Ray Crystallography*, edited by J. A. Ibers and W. C. Hamilton (Kynoch, Birmingham, England, 1974), Vol. IV, p. 47.
- <sup>68</sup>This follows from the asymptotic behavior  $n(\omega) - 1 = -\frac{1}{2} \omega_p^2/\omega^2$ , and Eq. (2.1).
- <sup>69</sup>J. R. Beattie, *Philos. Mag.* **46**, 235 (1955); see, also, J. R. Beattie and G. K. T. Cahn, *Philos. Mag.* **46**, 222 (1955); **46**, 989 (1955).
- <sup>70</sup>A. P. Lenham and D. M. Treherne, *J. Opt. Soc. Am.* **56**, 752 (1966).
- <sup>71</sup>J. N. Hodgson, *Proc. Phys. Soc. London, Sect. B* **68**, 593 (1955).
- <sup>72</sup>For a survey, see H. Raether, *Springer Tracts on Modern Physics* **38**, 84 (1965), and *Proceedings of the IV International Conference on Vacuum Ultraviolet Radiation Physics*, edited by E. E. Koch, R. Haensel, and C. Kunz (Vieweg, Braunschweig, 1974), p. 591.
- <sup>73</sup>Electron-energy-loss spectra have been employed to



- calculate the ultraviolet spectra of a number of substances. See, for example, R. E. LaVilla and H. Mendlowitz, *Phys. Rev. Lett.* **9**, 149 (1962); *J. Phys. (Paris)* **25**, 114 (1964); *Appl. Opt.* **4**, 955 (1965), and **6**, 61 (1967); and *J. Appl. Phys.* **40**, 3297 (1969). In general, this requires the normalization of the energy-loss function with the  $f$ -sum rule because of the lack of absolute measurements. In all cases known to the authors the effects of core polarizability on the  $f$  sum has been neglected in these calculations. (See the discussion of Eq. (18), Ref. 5). The present work indicates that this neglect of core polarizability in aluminum leads to 7–8% error in the normalization.
- <sup>74</sup>D. Pines, *Elementary Excitations in Solids* (Benjamin, New York, 1963).
- <sup>75</sup>See, for example, N. Swanson and C. J. Powell, *Phys. Rev.* **167**, 592 (1968). A brief review of complications in energy-loss spectra away from the plasma resonance is given in C. Colliex, V. E. Cosslett, R. D. Leapman, and P. Trebbia, *Ultramicroscopy* **1**, 301 (1976).
- <sup>76</sup>P. C. Gibbons (private communication). See also, P. C. Gibbons, S. E. Schnatterly, J. J. Ritsko, and J. R. Fields, *Phys. Rev. B* **13**, 2451 (1976).
- <sup>77</sup>M. Urner-Wille and H. Raether, *Phys. Lett.* **58A**, 265 (1976).
- <sup>78</sup>E. Petri and A. Otto, *Phys. Rev. Lett.* **34**, 1283 (1975).
- <sup>79</sup>T. Kloos, *Z. Phys.* **265**, 225 (1973).
- <sup>80</sup>P. Zacharias, *Z. Phys.* **256**, 92 (1972).
- <sup>81</sup>J. Geiger and K. Wittmaack, *Z. Phys.* **195**, 44 (1966).
- <sup>82</sup>G. T. Meaden, *Electrical Resistance of Metals* (Plenum, New York, 1965).
- <sup>83</sup>*Handbook of Chemistry and Physics*, 58th ed., edited by R. C. Weast, (CRC Press, Cleveland, 1977).
- <sup>84</sup>J. R. Beattie, *Physica (Utrecht)* **23**, 898 (1957).
- <sup>85</sup>A. I. Golovashkin, G. P. Motulevich, and A. A. Shubin, *Zh. Eksp. Teor. Fiz.* **38**, 51 (1960) [*Sov. Phys.-JETP* **11**, 38 (1960)].
- <sup>86</sup>To account for the contribution of processes beyond 10 keV a power-law extrapolation  $\kappa(\omega) \propto \omega^{-4}$  was employed. Between 10 keV and 30 or 40 keV, the  $\kappa(\omega)$  data accurately follow the  $\omega^{-4}$  behavior. Beyond 40 keV,  $\kappa(\omega)$  decreases somewhat more rapidly, but the region beyond 40 keV makes such a small contribution to  $n_{\text{eff}}(\omega)$  that extrapolation errors in this region are negligible. See Ref. 11.
- <sup>87</sup>The values reported here supersede the preliminary values reported in Ref. 5.
- <sup>88</sup>Y. Sagiura, *Philos. Mag.* **4** (7), 495 (1927); R. de L. Kronig and H. A. Kramers, *Z. Phys.* **48**, 174 (1928). For a modern review see U. Fano and J. W. Cooper, *Rev. Mod. Phys.* **40**, 441 (1968), Sec. 4.
- <sup>89</sup>See, for example, D. Y. Smith and D. L. Dexter, in *Progress in Optics*, edited by E. Wolf (North-Holland, Amsterdam, 1972), Vol. X, Sec. 3.2; F. Wooten, *Optical Properties of Solids* (Academic, New York, 1972).
- <sup>90</sup>F. Herman and S. Skillman, *Atomic Structure Calculations* (Prentice-Hall, Englewood Cliffs, N. J., 1963).
- <sup>91</sup>Similar arguments are made for the contact hyperfine interaction in the case of the knight shift. See, for example, W. D. Knight, in *Solid State Physics*, edited by F. Seitz and D. Turnbull (Academic, New York, 1956), Vol. 2, p. 93.
- <sup>92</sup>J. L. Dehmer, *J. Chem. Phys.* **56**, 4496 (1972).
- <sup>93</sup>The loss of oscillator strength of the 1s core level has been noted previously. See Ref. 2.
- <sup>94</sup>G. B. Bandopadhyaya and A. T. Maitra, *Philos. Mag.* **21**, 869 (1936).
- <sup>95</sup>R. D. Hill, *Proc. R. Soc. London, Ser. A* **161**, 284 (1937).
- <sup>96</sup>A. Balzarotti, A. Bianconi, and E. Burattini, *Phys. Rev. B* **9**, 5003 (1974).
- <sup>97</sup>A. Balzarotti, A. Bianconi, E. Burattini, M. Piacentini, G. Strinati, M. Grandolfo, and R. Habel, *Proceedings of the IV International Conference on Vacuum Ultraviolet Radiation Physics*, edited by E. E. Koch, R. Haensel, and C. Kunz (Vieweg, Braunschweig, 1974), p. 458.
- <sup>98</sup>R. K. Hart, *Proc. R. Soc. London, Ser. A* **236**, 68 (1956); B. Feuerbacher, M. Skibowski, W. Steinmann, and R. P. Godwin, *J. Opt. Soc. Am.* **58**, 137 (1968).
- <sup>99</sup>(a) O. S. Heavens, *Optical Properties of Thin Solid Films* (Dover, New York, 1965); (b) L. I. Maissel and M. H. Francombe, *An Introduction to Thin Films* (Gordon and Breach, New York, 1973).
- <sup>100</sup>H. A. Bethe, *Handbuch der Physik*, edited by H. Geiger and K. Scheel (Springer, Berlin, 1933), Vol. 24, Pt. 1, p. 491.
- <sup>101</sup>U. Fano, *Phys. Rev.* **103**, 1202 (1956).
- <sup>102</sup>For a review see U. Fano, in *Annual Review of Nuclear Science*, edited by E. Segrè, G. Friedlander, and H. P. Noyes (Annual Reviews, Palo Alto, 1963), Vol. 13, p. 1.
- <sup>103</sup>M. Inokuti and J. E. Turner, in *Proceedings of the Sixth Symposium on Microdosimetry, Brussels, May, 1978*, edited by J. Booz and H. G. Ebert (Harwood Academic, London, 1978), p. 675.
- <sup>104</sup>J. L. Dehmer, M. Inokuti, and R. P. Saxon, *Phys. Rev. A* **12**, 102 (1975).
- <sup>105</sup>H. Bichsel and E. A. Uehling, *Phys. Rev.* **119**, 1670 (1960).
- <sup>106</sup>J. E. Turner, P. D. Roecklein, and R. B. Vora, *Health Phys.* **18**, 159 (1970).
- <sup>107</sup>C. Tschalär and H. Bichsel, *Phys. Rev.* **175**, 476 (1968).
- <sup>108</sup>The total contribution to  $I$  from 10 keV to infinity is 3.1 eV; calculations using a variety of different extrapolations indicate an uncertainty in this value of much less than 1 eV.
- <sup>109</sup>T. Kloos, *Z. Phys.* **208**, 77 (1968).
- <sup>110</sup>The Stern rule,  $\int_0^\infty \omega \kappa(\omega) [n(\omega) - 1] d\omega = 0$ , is obtained by eliminating the plasma frequency between the  $f$ -sum rules for  $\epsilon_2$  and  $\kappa$ .